Seismological constraints on the source mechanism of the damaging seismic event of August 21, 2017 on Ischia island (Southern Italy)

Thomas Braun[1†], Daniela Famiani[1], and Simone Cesca[2]

[1]Istituto Nazionale di Geofisica e Vulcanologia, Sezione di Roma1, Via di Vigna Murata 605, 00143 Rome, Italy.

[2]GFZ German Research Center for Geosciences, Telegrafenberg, D-14473 Potsdam, Germany.

Corresponding author: Thomas Braun (thomas.braun@ingv.it)

† Seismological Observatory, Arezzo, Italy

Key words: Ischia earthquake, full moment tensor solution, rotated spectra

Abstract

On August 21, 2017, a M_D4.0 earthquake struck Ischia island, in the Tyrrhenian Sea off the coast of Naples, Italy. In spite of its modest magnitude, the earthquake caused two deaths and severe building damage on the northern side of the island. Initial hypocenter locations based on arrival times were highly uncertain and several proposed moment tensor solutions were inconsistent. These contradictory observations prompted a new calculation of the earthquake parameters with alternative methods. Our new approach, based on the determination of P-wave particle motion, evaluation of rotated spectra, and accurate calculation of S-minus-P travel time yields a hypocentral depth of 2 km and a location in the same area as the devastating seismic event that struck Ischia in 1883. We invert the moment tensor for a best-fitting double couple (DC), obtaining a M_w 3.9, with a normal mechanism, and an optimal depth of 8 km. Calculation of the full moment tensor results in: (i) 36% negative isotropic component and 26% negative CLVD components, (ii) a better fit at a more shallow source depth than for the corresponding DC, and (iii) a magnitude estimate of M_w 4.1. Modeling of the waveform and the first motion recorded in Ischia's station IOCA predicts, however, a negative polarity, in disagreement with the observation. We therefore suggest a complex rupture process, with an initial shallow normal faulting event that triggered a subsequent shallow underground collapse.

1 Introduction

Although in-depth investigations of moderate earthquakes are not generally warranted, a recent earthquake on Ischia, a small volcanic island located 33 km southwest of Naples (Southern Italy), is a worthwhile exception due to the striking discrepancy between the macroseismic intensity and the magnitude. On August 21, 2017, Ischia was struck by a seismic event of M_D 4.0 that provoked significant shaking and severe damages including unfortunately

two victims. In a dramatic rescue operation, three children were recovered alive under the rubble of a collapsed building (BBC, 2017, NYT, 2017, Telegraph, 2017). The incongruity between damage and magnitude cannot be only explained by local site effect or especially vulnerable constructions, but may also be influenced by particular characteristics of the seismic source.

The first automatic hypocenter location at INGV was off-shore (ca. 5 km N of San Montano; *SM* in Figure 1) - at a standard crustal depth of 10 km - in the area between Ischia island and the Italian Peninsula. Relocation of this seismic event confirmed a shallow hypocenter (ISIDe, 2016), in proximity to the observed maximum damage intensities. The calculated magnitudes of M_L 3.6, M_w 3.9 and M_D 4.0 (http://cnt.rm.ingv.it/event/16796811) seemed to be at odds with the high macroseismic intensity (hereafter reported as I_{EMS} – the Intensity of the European Macroseismic Scale; EMS, 1998).

While the coastal area of Marina di Casamicciola (*MC* in Figure 1) was less affected (I_{EMS}), the upper part of Casamicciola Terme (*CMRZ* in Figure 1) showed the most severe earthquake damage (I_{EMS} 7–8); such significant local variations are probably due to the diverse quality of construction (Azzaro et al., 2017). The majority of the houses are made of bricks, blocks of tufa and squared stone, without any structural reinforcement, such as tie rods or armoring irons. The damage appeared as cross cracks, loss of verticality and overturning of walls, ejection of edges, partial and a few total collapses. Reinforced concrete buildings had only minimal non-structural damage and in just a few cases. The complexity of the observed damage justified the assignment of I_{EMS} 8 to the Red Zone (*CMRZ* in Figure 1) of Casamicciola Terme (Azzaro et al., 2017). Differential SAR revealed a vertical deformation of 4 cm in the adjacent area SW of Casamicciola Terme immediately after the August 21, 2017 earthquake (Figures 1,5; after De Novellis et al., 2018)

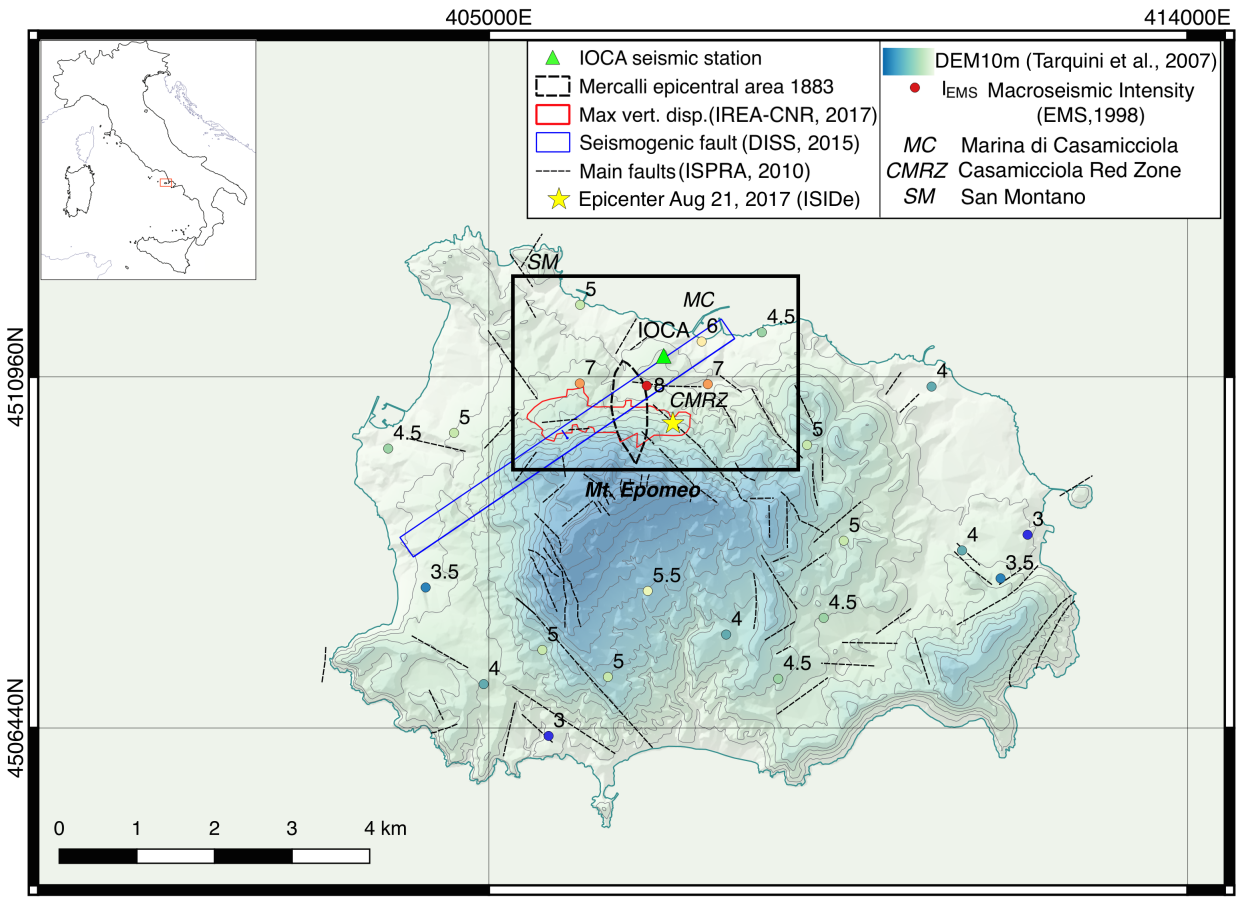

Figure 1: *Map of Ischia Island, showing the epicenter of August 21, 2017 (yellow star), the seismic station IOCA (green triangle), the area of maximum deformation (red curve), the epicentral area of 1883 (rugby ball shaped area; Mercalli, 1884), the main faults (dashed black lines) and the position of the seismogenic source (blue rectangular area). Numbers indicate macroseismic intensity (Azzaro et al., 2017) expressed in EMS values (EMS, 1998).*

The disagreement between the observed maximum macroseismic intensity and seismic energy seems to be related to the particular seismotectonics and geological situation of the volcanic island. This is not the first time that a local seismic event caused damages at Ischia that were much stronger than expected, given the moderate magnitude: On July 28, 1883, Ischia was struck by an earthquake that caused more than 2300 deaths and severe damage in the northern part of the island, near the small town of Casamicciola (rugby-ball-dashed area Figure 1 after

Mercalli, 1884; Palmieri and Oglialoro, 1884; Cubellis and Luongo, 1998; Carlino et al., 2010). For this event the "Italian catalogue of strong earthquakes" (CFTI (Guidoboni et al., 2007) reports a maximum intensity of I_{max}=X (MCS) and an "equivalent" intensity Magnitude M_e 5.8, estimated using the method of Bakun and Wentworth (1997). If we follow the approach of Wells and Coppersmith (1994), we find that the expected equivalent rupture length of a seismic event of M_e 5.8 ranges between 10 - 15 km, depending on the fault width. Such a fault dimension is not compatible with the reported damage pattern. By reconstructing the linear dimensions of the seismogenic source, Cubellis and Luongo (1998) proposed a fault length of 2 km for the 1883 earthquake and a corresponding magnitude range of $4.3 \leq M_w \leq 5.2$. In the most recent version of the "Parametric Catalog of Italian Earthquakes" (CPTI) the moment magnitude of the July 28, 1883 event was therefore downgraded to M_w 4.26 ± 0.5 (Rovida et al., 2016).

Another calculation of the fault dimension and seismic potential was proposed in the "Database of Individual Seismogenic Sources" (DISS-Working-Group, 2015) resulting in a 5 km x 3.5 km ENE-WSW-striking sub-vertical fault (ID: ITIS 068, ITCS085), and a seismic event with a maximum magnitude of M_w 5.4 (blue rectangular area in Figure 1).

The main objectives of this paper are to analyze the 2017 Ischia earthquake, trying to account for the disagreement between the high maximum macroseismic intensity and the relatively low magnitude, and to clarify the contradictory information on the source parameters calculated. This calculation is biased by the exclusive use of land-based stations and of a non-specific regional 1-D velocity model. To this end, we relocate the hypocenter by a single station method – using an *ad-hoc* velocity model - and calculate moment magnitude and source mechanism by inversion of the full moment tensor (using regional seismic data from the Italian Seismic Network – ISN).

2 Geological framework

Ischia island is a volcano, active over the last 150ky (Della Seta et al., 2012; Vezzoli 1988). The widespread presence of volcanic rocks, epiclastic deposits and subordinate terrigenous sediments reflects the complex sequence of alternating constructive and destructive phases of the volcanic edifice (Della Seta et al., 2012). The main recent volcano-tectonic event was the resurgence of the caldera after the explosive eruption (55ky BP) and deposition of the Mt. Epomeo Green Tuff (Acocella et al., 1999; Carlino, 2012). A maximum uplift of 900 m (Della Seta et al., 2012; Orsi et al., 1991) of the caldera floor is testified by the presence of marine sediments outcropping in the inner part of the island. The resurgent block is the central part of the island, has a polygonal shape, and is bordered, in its northern part (Mt. Epomeo in Figure 1), by a high angle inward-dipping fault (Acocella and Funiciello, 1999; Molin et al., 2003). The uplift of the block seems to be connected to the intrusion of a magmatic body at shallow depths (2 km) below the surface, and be responsible for the gravimetric and geothermic anomalies observed in this area (Carlino, 2012; Capuano et al., 2015). Cubellis and Luongo (1998) and Carlino et al. (2006) report that - due to the high geothermal gradient - the seismogenic volume (brittle regime) is confined in the upper 2 - 2.5 km of the crust.

3 Hypocenter determination

The location of earthquakes that occur in coastal areas or off-shore is a challenge. The lack of station coverage, in addition to the use of non-realistic 1D velocity models, introduce trade-offs among epicentral location, focal depth and origin time. Ocean bottom seismometers could generally be helpful to reduce the azimuthal gap and improve the location accuracy for these events (e.g.: Dahm et al., 2002; Sgroi et al., 2006), but are currently not installed in the area.

The first automatically calculated epicenter of the 2017 Ischia earthquake was located some kilometers off-shore, at a standard depth of 10 km. It quickly became obvious that the off-shore location was in strong contradiction with the pattern of the observed damage (Figure 1). In fact, the intensity pattern, narrow, concentric and slightly elongated in E-W direction (Azzaro et al., 2017), suggested a very shallow hypocentral depth. A re-calculation, based on additional data from local analog off-line seismic stations, established a hypocenter depth of 1.7 km about 1 km SSW of the center of the small town of Casamicciola (*CMRZ* in Figure 1). The associated origin time and coordinates reported by the "Italian Seismological Instrumental and Parametric Database" (ISIDe, 2016) are:

2017-08-21; 18:57:51.260 (UTC); Lat.: 40.739 N; Lon.: 13.903E; depth: 1.7 km

Although this hypocentral location is much more compatible with the damage pattern than the first one, we tried to improve it further by applying a detailed analysis on the seismogram from local station IOCA (Figure 1). This analysis involved the calculation of particle motions and azimuthal provenance of spectral energy.

To relocate the event with one 6-channel station (IOCA), we estimate the direction of seismic energy, from the azimuthal distribution of spectral energy (Wathelet et al., 2008) and calculate the rotated spectra on the unsaturated acceleration traces for different window lengths.

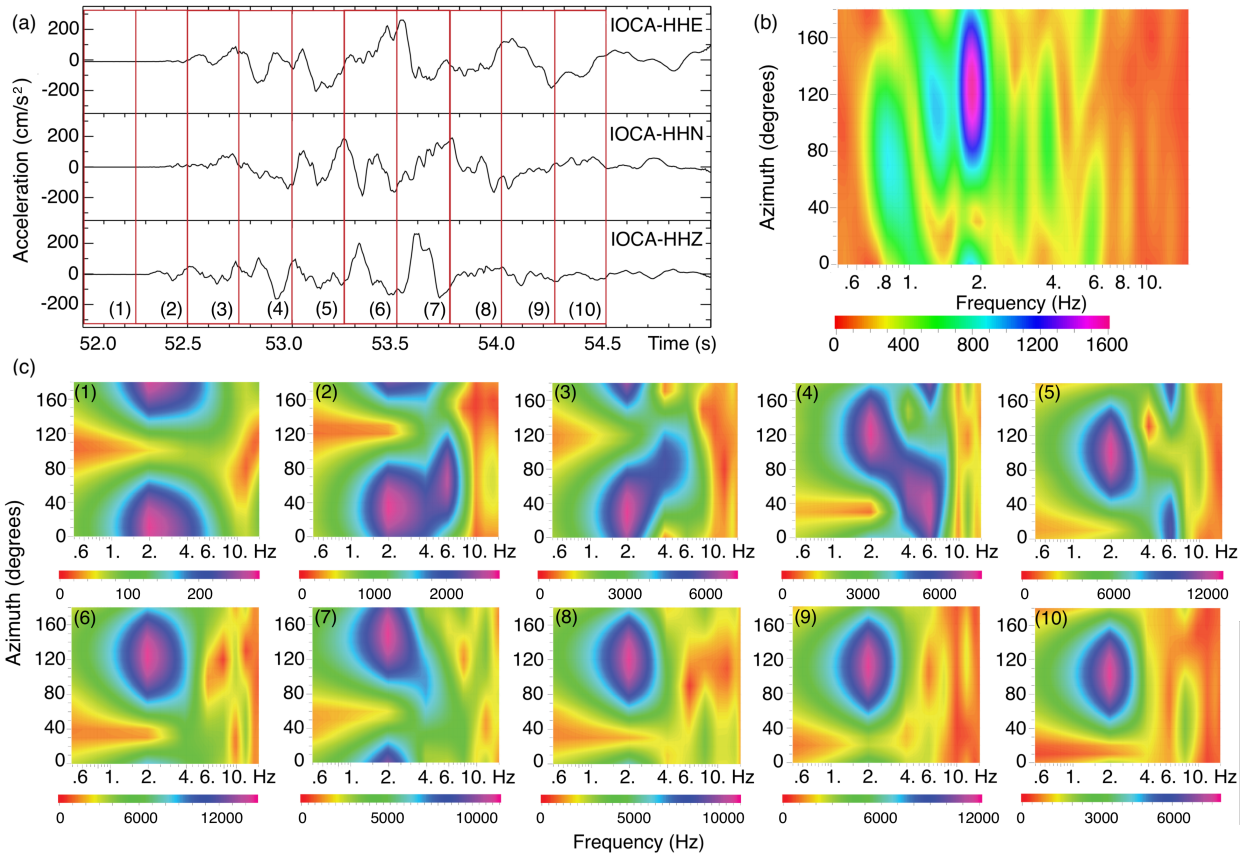

Figure 2: *(a) Accelerometric traces of the Ischia event recorded at IOCA; (b) rotated spectra calculated for the entire 3 s time window; (c) temporal variations of the azimuthal distribution of spectral energy recorded for the ten-time windows indicated in (a). Color bars indicate the spectral amplitude of the analyzed time window.*

The rotated spectrum, calculated for the entire 3s-time window of the seismogram (Figure 2a), reveals a mean maximum at 120°N for the frequency of 2 Hz (Figure 2b). This type of calculation always includes a 180° ambiguity. Spectral ratios from noise samples recorded at station IOCA, reveal a strong local amplification (up to factor H/V=8) for the frequency range between 1 and 3 Hz (GdL-INGV, 2017), indicating that in this specific frequency band there is a clear directionality for the same azimuth (120°N), the same as the one calculated for the P-phase of the 2017 Ischia event. This observation suggests that the seismic energy direction of arrival on the horizontal components may be influenced by a local site effect.

147 To evaluate the rotated spectra separately for the P- and S-phase, we divided the trace in
148 ten time windows of 0.5 s duration each (Figure 2a), with a respective overlap of 0.25 s. Figure
149 2c show the temporal variations of the rotated spectra for the single time windows (numbered
150 from 1–10): the first three time windows (corresponding to the P-phase) show that most of the
151 energy comes from 30°, which we interpret as backazimuth of the P.wave. After the fourth
152 window (S-phase) the direction of the dominant 2 Hz signal turns to 120°N, probably due to
153 resonance effects of the site and phase conversions.

154 As a next step we assess the polarization of the P-wave particle motion (Figure 3). We
155 observe clear positive onsets on all three components and a strongly linearly polarized P phase
156 motion, with NNE-SSW horizontal particle motion. These observations are in agreement with
157 the spectral analysis, and furthermore resolve the backazimuth ambiguity. Particle motions
158 suggest a backazimuth of ~215° and an incidence angle of ~20° with respect to the vertical
159 direction.

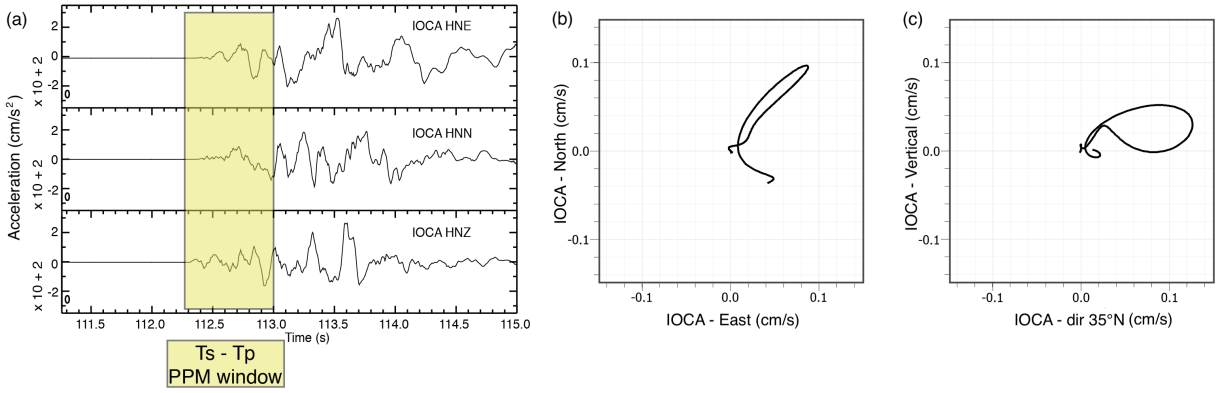

160

161 ***Figure 3:*** *(a) three-component accelerometric traces and the particle motion of the P-wave in*
162 *(b) the horizontal (N-E) and (c) the vertical-radial (35°N) plane.*

163

164 The observed S-minus-P travel time difference can be used to estimate the hypocentral
165 distance d, using the simple relation:

166 $$d = (t_s - t_p) \cdot v_p \cdot v_s/(v_p - v_s) = (t_s - t_p) \cdot c = 0.8 \cdot c \qquad (1)$$

167 d depends on the local geological situations of the volcanic island, where v_p and v_s are
168 significantly lower than standard, and their ratio may differ from the classical value $v_p/v_s = 1.73$.

169 We derived the P-wave velocity from a 3D-model calculated through tomographic
170 inversion (Capuano et al., 2015). P-velocities of $v_p = 1.5$ km/s and 3.1 km/s are reported for the
171 first two layers (0 - 900 m, 900 - 2500 m), respectively. Thus, we can assume a mean P-velocity
172 of 2.3 km/s for the upper 2.5 km, and consequently c varies between $1.92 \leq c \leq 3.29$ for $1.7 <$
173 $v_p/v_s < 2.2$, and the hypocentral distance ranges between 1.53 km $< d <$ 2.63 km (Figure 4).

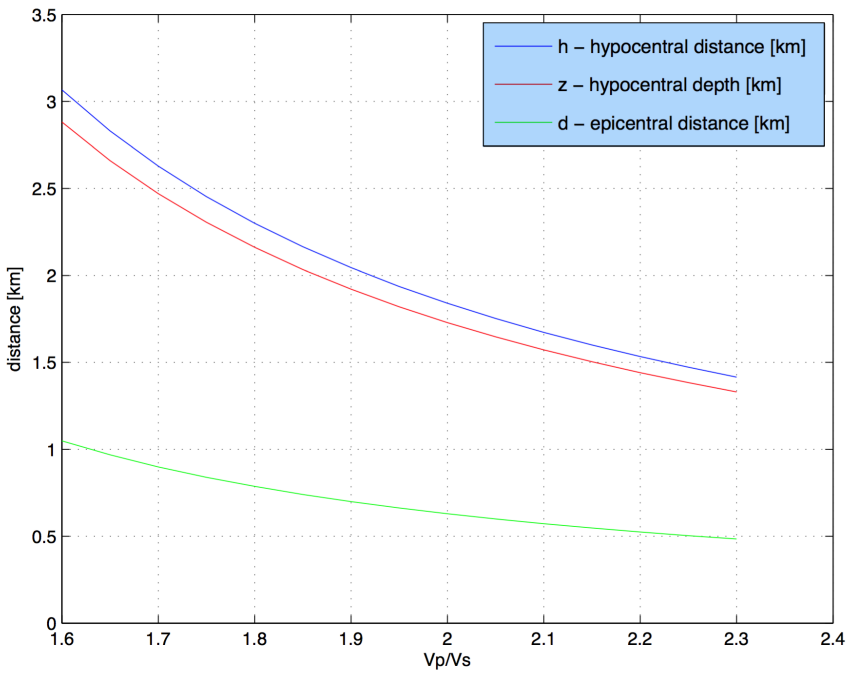

174

175 ***Figure 4:*** *Hypocentral depth (z), epicentral distance (d) and hypocentral distance (h) as function*
176 *of v_p/v_s (assuming $v_p = 2.3$ and $t_s - t_p = 0.8$ s).*

177

178 We constrain the relative hypocentral location with respect to station IOCA by combining
179 the information about the S-minus-P differential time (t_s - t_p = 0.8 s), the backazimuth (215°) and
180 the incidence angle (20°). The resulting depth z, hypocentral h and epicentral distance e for
181 various realistic v_p/v_s-ratios are shown in Figure 4. According to formula (1) the resulting
182 hypocentral h and epicentral distances e, as well as the depth z, depend on the v_p/v_s-ratio.
183 Assuming an average P wave velocity of v_p = 2.3 km/s, but v_s being unknown, we varied the
184 v_p/v_s-ratios from to 1.6 to 2.3.

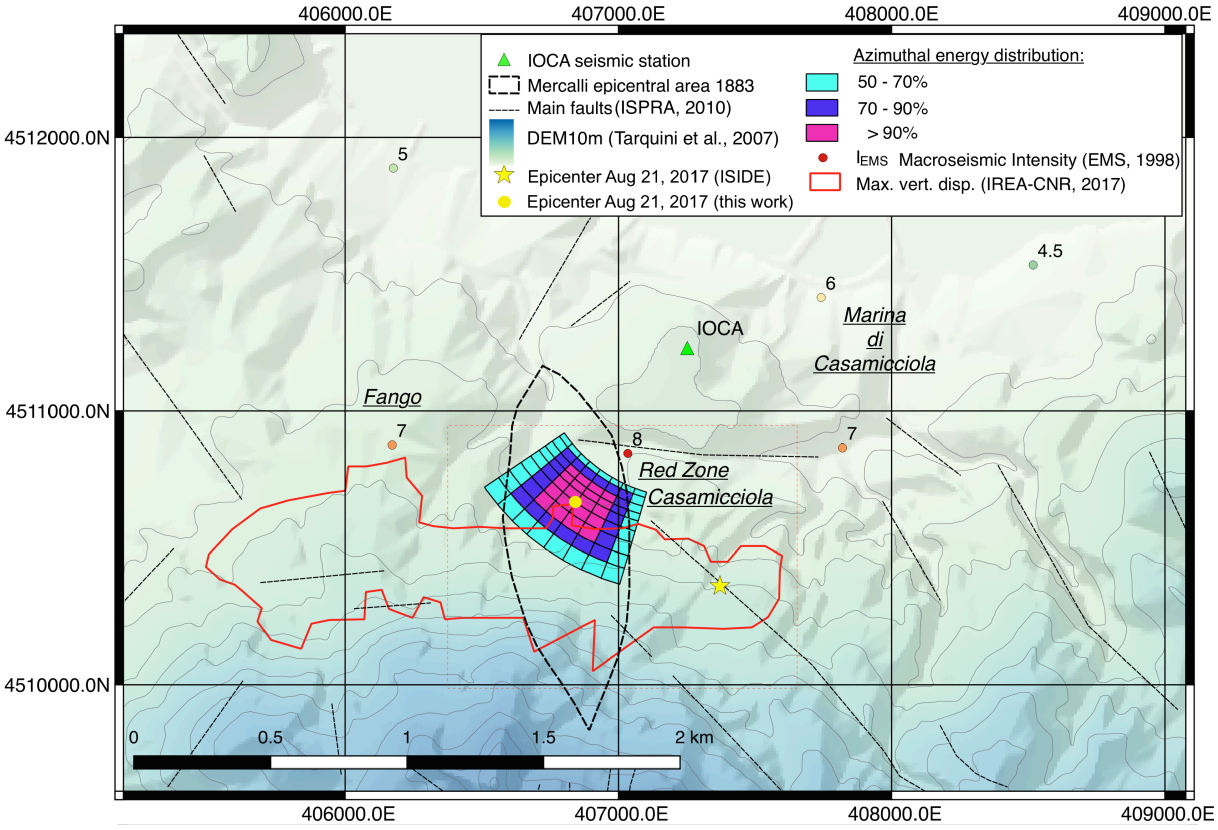

185

186 ***Figure 5:*** *Azimuthal energy estimate of the M_D 4.0 Ischia epicenter of August 21, 2017, as*
187 *derived in the present study.*

188 Figure 5 shows the map representation of the results shown in Figures 2, 3, 4. The
189 colored area depicts the location probability for the distance range of 1.53 km < d < 2.63 km and

an azimuthal range from 215°N ± 20°, thus obtaining a depth 1.92 km and an average epicenter location ~700 m SSW of IOCA at Latitude 40.74169 N and Longitude 13.89652 E.

If we compare the results obtained with the data from IOCA to the location reported by ISIDe (2016) (yellow star in Figures 1 and 5), we find that the epicentral distance is very similar, while the backazimuth is rotated towards SW by 20°. Figure 5 shows that the epicentral zone (purple) determined in this is study is (i) located at the northern rim of the red-encircled area where a 4 cm negative deformation (subsidence) found by satellite interferometry was observed immediately after the August 21, 2017 earthquake (De Novellis et al., 2018) and (ii) falls exactly in the rugby-shaped epicentral area, as first outlined by Mercalli (1884).

4 Full moment tensor inversion

A number of discrepant focal mechanism solutions have been proposed for the 2017 Ischia earthquake, based on time domain regional moment tensor inversion (Figure 6, from GdL-INGV, 2017). We consider three reference solutions, based on the following methods: RCMT-Regional Centroid Moment Tensor (Pondrelli et al., 2006), Time Domain Moment Tensor - TDMT (Scognamiglio et al., 2009), and a method developed by the Saint Louis University – SLU (Herrmann et al., 2011). These double couple (DC) solutions reveal very different mechanisms and orientations (Figure 6).

The RCMT solution is characterized by an oblique mechanism (strike-slip to normal faulting); the TDMT solution also shows an oblique mechanism, with a different orientation and potential planes oriented NE-SW and NNE-SSW. Finally, the SLU-solution corresponds to pure normal faulting, with E-W orientation. Besides, having a common normal faulting component, the focal mechanisms show very different orientations. Moment magnitude estimates ($3.8 \leq M_w$

≤ 4.0) and source depth estimation (3 - 8 km) are in better agreement. It is worth noting that accuracy in the estimation of the centroid depth is often limited by the range of frequency used for moment tensor inversion, such that the moment tensor depths provide overall evidence of a shallow source, which we estimated more accurately at 2 km using local data.

In addition to differences in the implementation of the regional moment tensor inversions technique and in the adopted velocity models, the large discrepancy among the proposed focal mechanisms can be attributed to two main factors: the observation capability and the seismic source depth. The first factor concerns the geometry of the station network , which determines the azimuthal coverage of the offshore epicenter and the range of epicentral distances. In general, there is an intrinsic heterogeneity of the station distribution, denser along the Italian peninsula and less dense on the islands. This factor, in the absence of OBSs, can negatively affect the moment tensor resolution (e.g. Domingues et al., 2013). The second factor is the very shallow depth of the seismic source, which can strongly affect the resolution of certain moment tensor components (Cesca et al., 2017).

Following the method described in Cesca et al. (2013), we performed spectral and waveform-based moment tensor inversions to determine the seismic source geometry, by assuming a pure double couple and a full moment tensor model and using the on-shore stations of the Italian Seismic Network (ISN) located at regional distances (Figure 6). In comparison to former inversions, we use a greater number of seismic stations (up to 14 stations) to reduce the azimuthal gap (down to ~200°). The smallest azimuthal gap is obtained in the RCMT solution, although it mostly uses stations at larger distances (see Figure 6, top right map inset). Furthermore, the full waveform amplitude spectra inversion is less sensitive than a time domain approach to the accuracy of the velocity model (we use a regional model based on the

CRUST2.0 database; Bassin et al., 2000), and allows us to invert higher frequency data up to 0.08 Hz. Thanks to the improvement in stations' geometry and the fit of high frequency data we can better resolve the centroid depth and the moment tensor. We first invert for a double couple (DC), obtaining a M_w 3.9 normal fault with a best fit solution at a depth of 8 km. This solution is in reasonably good agreement with the one calculated by TDMT (Figure 6).

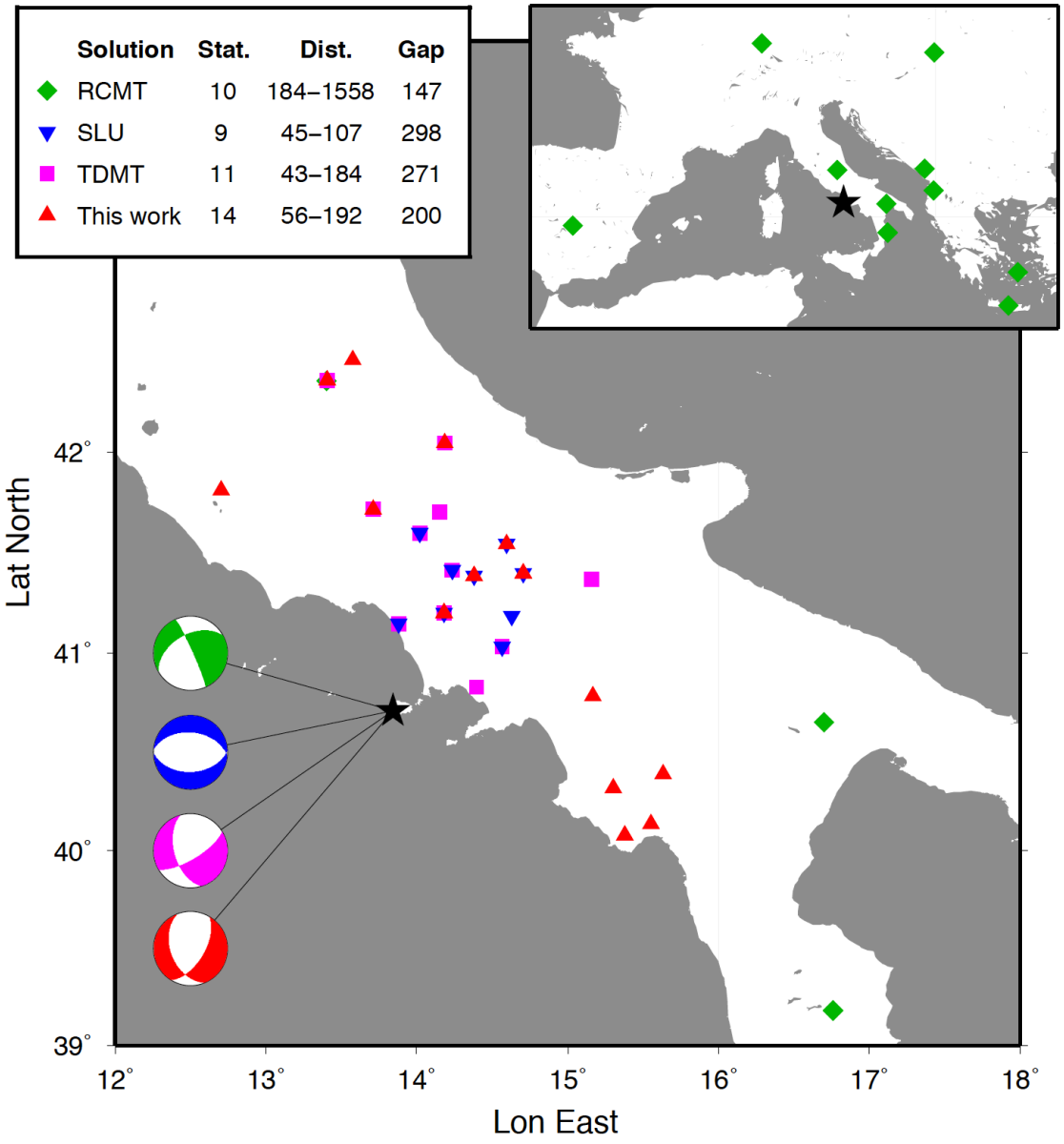

Figure 6: *Comparison of moment tensor solutions by: RCMT (green, best DC source), SLU (blue, best DC source), TDMT (purple, DC component of the best deviatoric MT) and this work (red, best DC source). The map shows the stations used by different authors (different symbols, colors according to the focal spheres); with the upper right map inset showing stations at regional distances used by RCMT. The upper left inset lists the number of used stations, range of epicentral distances and azimuthal gap.*

We additionally perform a full moment tensor inversion, to assess the presence and robustness of isotropic and CLVD components. Comparative results of full MT and DC inversions (Figure 7) demonstrate a large improvement of spectral and waveform fit, when a very shallow MT solution is chosen, at a depth of 2 - 4 km. The best fitting MT solution, for a depth of 4 km, is characterized by a significant negative isotropic component of 36% (contraction), a negative CLVD of 26% and a normal faulting DC component of 38%. The seismic moment amounts to $2.30 \cdot 10^{15}$ Nm, corresponding to a moment magnitude of M_w 4.1. The ~0.2 increase in M_w-magnitude, in comparison to the best DC solution and other reference solutions, can be mostly attributed to the non-DC term.

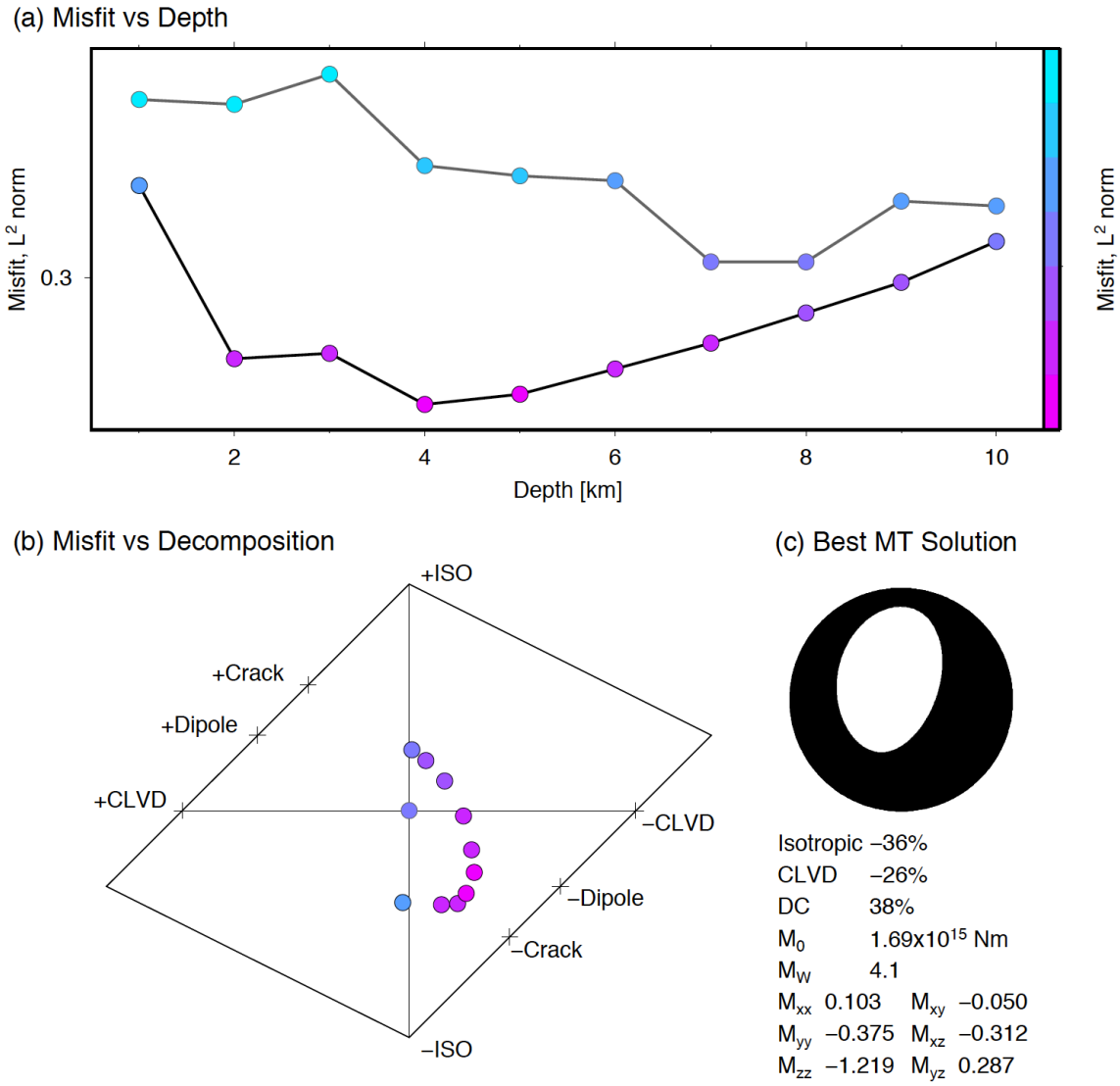

256

257 ***Figure 7:*** *DC and full MT solutions for the Ischia earthquake. (a) Comparison of amplitude*
258 *spectra fit (L2 norm) for different source depths, assuming a DC (gray line) and full MT (black*
259 *line) source model, the color bar denoting the misfit value. (b) Hudson plot representation of the*
260 *source type for full MT and DC solutions at different source depths: best fitting solutions show a*
261 *significant negative tensile component, a potential signature of a collapse process. (c) Best full*
262 *MT solution and related source parameters.*

263

5 Discussion and Conclusions

The examination of seismic events on Ischia island suggests that they cause damages which are spatially concentrated and greater than expected, given their moderate magnitude. A discrepancy between damaged and magnitudes was observed during the August 21, 2017 earthquake (I_{EMS} 8; Azzaro et al., 2017; M_w 4.1, this study), as well as the devastating July 28, 1883 earthquake (I_{max}=X (MCS); Guidobuoni et al., 2007; M_w 4.26 ± 0.5, Rovida et al., 2016).

Prompted by the inconsistencies of the arrival-times-based locations, we relocated the hypocenter of the 2017 earthquake by analyzing data from the 6-channel station IOCA (Figures 1, 5). The S-minus-P wave travel time of 0.8 s calculated by considering different v_p/v_s-ratios, resulted in epicentral/hypocentral distances ranging between 0.55 - 0.9 km and 1.6 - 2.6 km, respectively.

Calculation of the rotated spectra, combined with particle motion analysis indicated that the seismic energy of the P-phase reached IOCA from SSW (backazimuth 215°N±20°). The identified epicentral area is congruent with the one proposed by Mercalli (1884) for the July 28, 1883 earthquake. Furthermore, the 2017 earthquake seems to be located at the northern rim of the co-seismic vertical deformation field (maximum value of 4 cm in the red-encircled area) - as revealed by differential SAR (Figures 1 and 5). Our proposed hypocentral depth of 2 ± 0.5 km agrees with Carlino et al. (2006) who report the brittle regime to be confined in the upper 2 - 2.5 km of the crust.

Spectral and waveform-based moment tensor inversions were applied using ISN-data recorded at regional distances, following the approach of Cesca et al. (2013). In a first step, we inverted for a DC and obtained a solution with an M_w 3.9 normal fault and a best fit depth of 8 km, compatible with the one proposed using the TDMT (Figure 6). In order to check for the

combined contribution of isotropic and CLVD terms we performed an additional full moment tensor inversion. As shown in Figure 7, the spectral and waveform fit improve significantly if we assume a shallow source depth (2 - 4 km). The contribution of the non-DC-components leads to a ~0.3 distinct increase in M_w magnitude with respect to the best DC-solution. The difference of our approach and the TDMT, RCMT and SLU-solutions are that we use a higher number of stations for the inversion, which leads to a slightly smaller azimuthal gap. In addition, we use higher frequencies and calculate the full moment tensor, inverting also for both CLVD and isotropic components.

At first sight, the clear positive first motion onset observed at station IOCA seems to be incompatible with focal mechanism. In fact, the best models of the local waveforms and first motion onset observed at IOCA that include a 2-layered shallow structure (Capuano et al., 2015) and assume a focal depth of 2 km, our best DC and MT solutions, as well as other proposed solutions (Figure 7), predict a negative onset. We were able to reproduce the positive onset with our best DC model and a shallower source depth (1 km or less). Possible causes for the polarity mismatch at a shallow depth when using our best MT model are the low resolution of non-DC moment tensor components for shallow sources (Cesca and Heimann, 2018) and/or the inadequacy of the 1D velocity model at such small scale.

The 36% and 26% of negative isotropic component and negative CLVD components do not represent a pure closing tensile crack but a complex process, which could indicate the activation of a fault accompanied by a rapid subsidence. Therefore, to explain the polarity mismatch, we suggest an alternative hypothesis. In which a first shallow normal faulting event activated a collapse with failure on one of the high-angle normal fault which surrounds mainly the northern rim of the summit of Mt. Epomeo (Carlino, 2012; Capuano et al., 2015). This

collapse is compatible with the vertical deformation of 4 cm revealed by differential SAR in the adjacent area SW of Casamicciola Terme (Figures 1, 5; after De Novellis et al., 2017). Under this hypothesis, the first motion at IOCA is controlled by the triggering event, while the moment tensor solution depends on the radiation pattern of the complex rupture.

A very similar model was proposed for a complex seismic event in a copper mine in Poland (Rudzinski et al., 2016), where a small M_w 3.6 earthquake on an inverse fault triggered a successive energetic M_w 4.2 tabular collapse event, producing a significant discrepancy among the local scale focal mechanism solution based on first motion polarity and the regional scale moment tensor based on full waveform data.

We conclude that strong seismological evidences for a shallow collapse, confirmed by geodetic observations of 4 cm post-event vertical subsidence, and a narrow damage pattern, suggest that the August 21, 2017 seismic event on Ischia has been a repetition of the devastating earthquake of July 28, 1883.

Data and Resources

Regional seismic data were accessed through the repository of the Observatories and Research Facilities for European Seismology (ORFEUS) project (http://www.orfeus-eu.org/data.html) and the Italian Seismological Instrumental and Parametric Database (ISIDe), managed by INGV (http://iside.rm.ingv.it/standard/index.jspd). Routine moment tensor analysis of the Ischia event realized by RCMT - Regional Centroid Moment Tensor and TDMT - Time Domain Moment Tensor are available at (http://autorcmt.bo.ingv.it/QRCMT-online/E1708211857A.html) and (http://cnt.rm.ingv.it/event/16796811), respectively.

Accelerometric data of station IOCA were accessed through the repository (http://www.emsc.org). Regional moment tensor inversions were obtained with the Kiwi tools inversion platform (http://kinherd.org). The parameters of the seismogenic source ITIS 068 (ITCS085) refers to the Database of Individual Seismogenic Sources (http://diss.rm.ingv.it/diss/). Some of the figures were prepared using the Generic Mapping Tools package (Wessel and Smith, 1998) and QGIS software (QGIS Development Team, 2009).

Acknowledgments

We are grateful to Silvia Pondrelli for making available the RCMT data, to Stephen Monna for the accurate review of the English text, and to him and Giuliano Milana for useful suggestions. One of the coauthors (D.F.) was financed by DPC grant (INGV–DPC B2 2017 OB1 Task B) n° 0304-022.

References:

Acocella, V., R. Funiciello, 1999. The interaction between regional and local tectonics during resurgent doming: The case of the island of Ischia, Italy. *J. Volcanol. Geotherm. Res.* 88, 109-123.

Azzaro, R., S. Del Mese, G. Martini, S. Paolini, A. Screpanti, V. Verrubbi, and A. Tertulliani (2017). QUEST – Rilievo macrosismico per il terremoto dell'isola di Ischia del 21 agosto 2017. *Rapp. Int. INGV.* doi:105281/zenodo.849091.

Bakun, W.H., and C.M. Wentworth (1997). Estimating earthquake location and magnitude from seismic intensity data. *Bull. Seismol. Soc. Am.* **87**, 6, 1502-1521.

Bassin, C., G. Laske, and G. Masters (2000). The current limits of resolution for surface wave tomography in North America. Eos Trans. AGU 81, F897.

BBC (2017). http://www.bbc.com/news/world-europe-41007613

Capuano P., R. De Matteis, and G. Russo (2015). The structural setting of the Ischia Island Caldera (Italy): first evidence from seismic and gravity data. *Bull. Volcanol.* **77** (79). doi: 10.1007/s00445-015-0965-4.

Carlino, S. (2012). The process of resurgence for Ischia island (southern Italy) since 55 ka: the laccolith model and implications for eruptions forecasting. *Bull. Volcanol.* **74** (5), 947-961.

Carlino, S., E. Cubellis, G. Luongo, and F. Obrizzo (2006). On the mechanics of caldera resurgence of Ischia Island (southern Italy). In: C. Troise, G. De Natale, C.R.J. Kilburn (eds.), Mechanism of activity and unrest of large calderas. *Geological Society Special Publications*, **269**, London, 181-193.

Carlino, S., E. Cubellis, and A. Marturano (2010). The catastrophic 1883 earthquake at the island of Ischia (southern Italy): macroseismic data and the role of geological conditions. *Nat. Hazards* **52**: 231-247. doi: 10.1007/s11069-009-9367-2.

Cesca, S. and S. Heimann (2018). Challenges in Regional Moment Tensor Resolution and Interpretation. In: D'Amico S. (eds) Moment Tensor Solutions. Springer Natural Hazards. Springer, Cham. doi:10.1007/978-3-319-77359-9_7.

Cesca, S., A. Rohr, and T. Dahm (2013). Discrimination of induced seismicity by full moment tensor inversion and decomposition *J. Seismol*. doi: 10.1007/s10950-012-9305-8.

Cesca, S., S. Heimann, M. Kriegerowski, J. Saul, and T. Dahm (2017). Seismic analysis of nuclear explosions: what can we learn from the January 6 and September 2016 nuclear tests, North Korea? *Seismol. Res. Lett*. doi:10.1785/0220160139

Cubellis, E., and G. Luongo (1998). Il terremoto del 28 luglio 1883. Campo macrosismico e studio della sorgente. In: "Il terremoto del 28 luglio 1883 a Casamicciola nell'isola d'Ischia". *Servizio Sismico Nazionale, Istituto Poligrafico e Zecca dello Stato*, 101-110.

Dahm, T., M. Thorwart, E. Flüh, T. Braun, R. Herber, P. Favali, L. Beranzoli, G. D'Anna, F. Frugoni, and G. Smriglio (2002). Ocean bottom seismometers deployed in the Tyrrhenian Sea. *EOS, Transactions, A.G.U.,* **83**, 309 – 315.

Della Seta M., C. Esposito, G.M. Marmoni, S. Martino, A. Paciello, C. Perinelli, and G. Sottili, (2012): Geological constraints for a conceptional evolutionary model of the slope deformations affecting Mt. Nuovo at Ischia (Italy). *Ital. J. Eng. Geol. Environm*., **2**, 15-28. doi:10.4408/IJEGE.2015-02.O-04.

De Novellis, V., S. Carlino, R. Castaldo, A. Tramelli, C. De Luca, N. A. Pino, S. Pepe, V. Convertito, I. Zinno, P. De Martino, M. Bonano, F. Giudicepietro, F. Casu, G. Macedonio, M. Manunta, C. Cardaci, M. Manzo, D. Di Bucci, G. Solaro, G. Zeni, R. Lanari, F. Bianco, and P. Tizzani (2018). The 21 August 2017 Ischia (Italy) Earthquake Source Model Inferred From Seismological, GPS, and DInSAR Measurements. *Geophys. Res. Lett. 45*, 2193–2202. doi:10.1002/2017GL076336.

DISS-Working-Group (2015). Database of Individual Seismogenic Sources (DISS), Version 3.2.0: A compilation of potential sources for earthquakes larger than M 5.5 in Italy and surrounding areas. http://diss.rm.ingv.it/diss/. *Istituto Nazionale di Geofisica e Vulcanologia*. doi:10.6092/INGV.IT-DISS3.2.0.

Domingues, A., S. Custodio, and S. Cesca (2013). Waveform Inversion of Small to Moderate Earthquakes Located Offshore Southwest Iberia. *Geophys. J. Int.* doi: 10.1093/gji/ggs010.

EMS (1998). European Macroseismic Scale. In G. Grünthal (ed.) Conseil de l'Europe. *Cahier du Centre Européen de Géodynamique et de Séismologie*. Vol. 15.

GdL-INGV (2017). Rapporto di sintesi preliminare sul terremoto dell'isola di Ischia (Casamicciola) M4.0 del 21 agosto 2017 (6 settembre 2017). *Gruppo di lavoro sul terremoto dell'isola di Ischia*, *INGV*. doi: 10.5281/zenodo.886045.

Guidoboni, E., G. Ferrari, D. Mariotti, A. Comastri, G. Tarabusi, and G. Valensise (2007). Catalogue of Strong Earthquakes in Italy (461 B.C.-1997) and Mediterranean Area (760 B.C.-1500). *SGA Bologna*. http://storing.ingv.it/cfti4med/

Herrmann, R.B., L. Malagnini, and I. Munafò (2011). Regional moment tensors of the 2009 L'Aquila earthquake sequence. *Bull. Seism. Soc. Am.,* **101**, 975-993. doi: 10.1785/0120100184.

ISIDe (2016). Italian Seismological Instrumental and Parametric Database, version 1.0. http://iside.rm.ingv.it/standard. doi: 10.13127/ISIDe.

ISPRA (2010). ISPRA - Servizio Geologico d'Italia – Carta Geologica d'Italia – Progetto CARG – Foglio 464. Isola d'Ischia. *Litografia Artistica cartografica*, Firenze.

Mercalli, G. (1884). L'isola d'Ischia ed il terremoto del 28 luglio 1883. *Mem. Reg. Ist. Lombardo Scienze e Lettere*, **3** (6), 99-154.

Molin, P., V. Acocella, and R. Funiciello (2003). Structural, seismic and hydrothermal features at the border of an active intermittent resurgent block: Ischia island (Italy). *J. Volcanol. Geotherm. Res.* 121, 65-81.

NYT (2017): https://www.nytimes.com/2017/08/22/world/europe/italy-ischia-earthquake.html

Orsi, G., G. Gallo, and A. Zanchi (1991): Simple shearing block resurgence in caldera depressions. A model from Pantelleria and Ischia. *J. Volcanol. Geoth. Res*., **47**, 1-11.

Palmieri, L., and A. Oglialoro (1884). Sul terremoto dell'isola d'Ischia della sera del 28 luglio 1883. *Atti Reale Acc. Scienze Fis. Mat., Napoli*, **2**, 1.

Pondrelli, S., S. Salimbeni, G. Ekström, A. Morelli, P. Gasperini, and G. Vannucci (2006). The Italian CMT dataset from 1977 to the present. *Phys. Earth Planet. Int.*, **159** (3-4), 286-303, doi:10.1016/j.pepi.2006.07.008.

QGIS Development Team, 2009. QGIS Geographic Information System. Open Source Geospatial Foundation.

Rovida, A., M. Locati, R. Camassi, B. Lolli, and P. Gasperini (2016). CPTI15, the 2015 version of the Parametric Catalogue of Italian Earthquakes. *Istituto Nazionale di Geofisica e Vulcanologia.* doi:10.6092/INGV.IT-CPTI15.

Rudzinski, L., S. Cesca, and G. Lizurek (2016). Complex rupture process of the 19 March 2013, Rudna Mine (Poland) induced seismic event and collapse in the light of local and regional moment tensor inversion. *Seismol. Res. Lett.* 87(2), 11p. doi:10.1785/0220150150.

Scognamiglio, L., E. Tinti, and A. Michelini (2009). Real-time determination of seismic moment tensor for the Italian region. *Bull. Seismol. Soc. Am.*, **99** (4), 2223-2242.

Sgroi, T., T. Braun, F. Frugoni, and T. Dahm (2006). An improved seismicity picture of the Southern Tyrrhenian area by the use of OBS and land-based networks: the TYDE experiment. *Ann. Geophys.,* **49**, 801-817.

Tarquini, S., I. Isola, M. Favalli, F. Mazzarini, M. Bisson, M.T. Pareschi, and E. Boschi (2007). TINITALY/01: a new Triangular Irregular Network of Italy. *Ann of Geophys.*, 50, 407-425.

Telegraph (2017): https://www.telegraph.co.uk/travel/destinations/europe/italy/articles/ischia-earthquake-naples-travel-advice-italy/

Vezzoli, L. (1988): Island of Ischia. *Quaderni de "La Ricerca Scientifica"*, **114**, CNR, 133pp.

Wathelet, M., D. Jongmans, M. Ohrnberger, and S. Bonnefoy-Claudet (2008). Array performances for ambient vibrations on a shallow structure and consequences over Vs inversion. *J. Seismol.,* **12**, 1-19.

Wells, D.L., and K.J. Coppersmith (1994). New empirical relationships among magnitude, rupture length, rupture width, rupture area and surface displacement. *Bull. Seismol. Soc. Am.*, **84** (4), 974-1002.

Wessel, P., and W.H.F. Smith (1998). New improved version of Generic Mapping Tools released, *EOS Trans. AGU* **79**, 579.